

Energy relaxation due to magnetic impurities in mesoscopic wires: Logarithmic approach

O. Újsághy^a, A. Jakovác^a, and A. Zawadowski^{a,b}

^a*Budapest University of Technology and Economics,
Institute of Physics and Research group Theory of Condensed Matter
of Hungarian Academy of Sciences H-1521 Budapest, Hungary and*

^b*Research Institute for Solid State Physics, POB 49, H-1525 Budapest, Hungary*

(Dated: January 28, 2019)

The transport in mesoscopic wires with large applied bias voltage has recently attracted great interest by measuring the energy distribution of the electrons at a given point of the wire, in Saclay. In the diffusive limit with negligible energy relaxation that shows two sharp steps at the Fermi energies of the two contacts. Those steps are, however, broadened due to the energy relaxation which is relatively weak if only Coulomb electron-electron interaction is assumed. In some of the experiments the broadening is more essential reflecting an anomalous energy relaxation rate proportional to E^{-2} instead of $E^{-3/2}$ where E is the energy transfer. Later it has been suggested that such relaxation rate can be due to electron-electron interaction mediated by Kondo impurity which is, as it is known since a long time, singular in E . In the present paper the magnetic impurity mediated interaction is systematically studied in the logarithmic approximation valid above the Kondo temperature. In the case of large applied bias voltage Kondo resonances are formed at the steps of the distribution function and they are narrowed by increasing the bias. An additional Korringa energy broadening occurs for the spins by creating electron-hole pairs in the electron gas out of equilibrium. That smears the Kondo resonances, and the renormalized coupling can be replaced by a smooth but essentially enhanced average coupling and that enhancement can reach the value 8-10. Thus the experimental data can be described by formulas without logarithmic Kondo corrections, but with enhanced coupling. In certain regions of large bias, that averaged coupling depends weakly on the bias. In those cases the distribution function depends only on the ratio of the electron energy and the bias, showing scaling behavior. The impurity concentrations estimated from those experiments and other dephasing experiments can be very different. An earlier paper has been devoted to provide a possible explanation for that by considering the surface spin anisotropy due to strong spin-orbit interaction in the host which can hinder the motion of spins with integer spin value.

PACS numbers: 73.23.-b,72.15.Qm,71.70.Ej

I. INTRODUCTION

In the last few years the study of inelastic electron scattering mechanisms in mesoscopic metallic systems has attracted considerable interest both experimentally and theoretically. The motivation is to identify the mechanisms responsible for destroying the quantum coherence of the quasiparticles. In one kind of the experiments the dephasing time is determined from measurements of magnetoresistance^{1,2,3,4,5}, universal conductance fluctuation⁶, and Aharonov-Bohm oscillation in mesoscopic rings in magnetic fields⁴. In the other kind of experiments on short wires with large bias voltage the non-equilibrium distribution functions of the electron energies are measured^{7,8,9} which provides an indirect information about the energy relaxation of the electrons. The dephasing and energy relaxation are due to inelastic scattering processes, thus we can obtain information on those from these two kinds of experiments. The experiments were performed at very low temperatures (below about 1K) where the electron-phonon scattering is weak, thus the main inelastic processes are the electron-electron scattering and the scatterings by dynamical defects (e.g. magnetic impurities, two-level systems).

In this paper we investigate theoretically the energy re-

laxation due to magnetic impurities in thin metallic wires with large bias voltage. Our motivation is that there are many cases where deviations from the expectations of the theory of Coulomb electron-electron interaction by Altshuler, Aronov and coworkers¹⁰ were found. The Saclay group⁷ analyzing the experimental data suggested a phenomenological anomalous effective energy relaxation rate proportional to E^{-2} where E is the energy transfer. That differs from the one due to the Coulomb interaction which varies like $E^{-3/2}$. That anomalous relaxation rate was attributed to the presence of magnetic impurities either implanted or contained by the starting material as contamination or dynamical defects^{11,12,13,14,15,16}.

The main goal of our earlier paper³¹ has been to suggest a resolution of the discrepancy concerning the required magnetic impurity concentrations to fit the different experimental data and in some cases those discrepancies may reach the level of two orders of magnitude. Therefore, even the role of magnetic impurities was questioned in spite of the observed sensitivity on external magnetic field¹⁷. Having a thin wire the magnetic surface anisotropy¹⁸ has been taken into account in Ref. 31 which hinders the motion of the spin and in that way reduces the Kondo scattering. The previous theoretical works^{11,12,13,14,15,16}, however, showed the phenomena is

rather complex and it is very hard to separate and identify the role of the different effects. That is especially valid for the non-crossing approximation which is based on extensive numerical work^{13,15} and many details are hidden. The present paper is devoted to those problems, and the role of surface anisotropy has already been discussed in Ref. 31.

Considering the Kondo effect the different temperature and energy ranges have very different characters. Below the characteristic Kondo energy the Fermi liquid behavior is recovered. That range has been intensively studied even in the non-equilibrium situation in case of wires, but the situation in quantum dots shows strong similarities^{19,20}. The most difficult range is around the Kondo energy, while well above that perturbative approaches are appropriate, known as logarithmic approximation. The main idea is to apply perturbation theory and to collect the terms with the highest power of the characteristic logarithm in each order. That leading logarithmic approach is well established. It will be shown that most of the experiments fall in that range.

In case of non-equilibrium situation the voltage applied on the short wire plays crucial role which has to be incorporated into that scheme.

The applied voltage U occurs in two different ways:

(i) *Reduction of the Kondo temperature:* In a short wire in the diffusive limit with a weak energy relaxation the electron comes from one of the two contacts without energy loss. The distribution of those electrons is characterized by different Fermi energies which are split by the applied voltage, eU where e is the electronic charge. The Kondo effect arises from those regions where there are sharp changes in the energy distribution functions, thus at the two Fermi energies. At both places separate Kondo resonances develop, but the amplitudes of sharp changes in the distribution at both energies are reduced compared to the equilibrium case, where the change is the sum of those two. Therefore, in the wire the equilibrium Kondo temperature for the step with e.g. the lower energy is reduced at position x as^{14,16,21}

$$T_K(x) = \frac{T_K^{\frac{1}{1-x}}}{(eU)^{\frac{x}{1-x}}} \quad (1)$$

which is valid for $T_K < eU$ where x is measured in the units of the length of the wire L . The voltage U measures the energy range where the non-equilibrium electron distribution takes place. That reduction in T_K can be very essential, e.g. for $T_K = 0.3$ K, $eU = 0.3$ meV \sim 3 K, and $x = 0.5$, $T_K(x = 0.5) = 0.1T_K = 0.03$ K. Thus for a considerable voltage and for Kondo temperature in a typical range ($T_K = 0.1 - 1$ K) the reduced Kondo temperature is rather small compared to the energy scale eU playing role in the electronic transport. That ensures the applicability of the logarithmic approach as far as $T_K \ll eU$. In other cases, e.g. the non-crossing approximation must be applied^{13,15}.

(ii) *Enhanced Korringa relaxation rate:* the Korringa relaxation²² describes the impurity spin relaxation due

to electron-hole creations. The creation of those with almost zero energy can be only in the energy range where the sharp single-step ($T = 0$) electron distribution is modified. That can be achieved by raising the temperature or applying the voltage. In the latter case the extra relaxation rate is

$$\frac{\hbar}{2\tau_K} = 2\pi S(S+1)(\rho_0 J)^2 x(1-x)eU \quad (2)$$

at $T = 0$ where S is the spin of the impurity and $\rho_0 J$ is the dimensionless electron-impurity spin coupling. In the equilibrium case the Korringa relaxation rate is not part of the logarithmic approach, but $eU \gg T_K$ makes it non-negligible.

Namely, in the next to leading logarithmic approximation the real part of the pseudospin particle self-energy contains a single log which is even lost in the imaginary part. That log is not contained by the simple logarithmic approach. The effect of the imaginary part (the inverse lifetime of the spin) remains, however, very crucial. For spins there are different relaxation rates e.g. the T_1^{-1} and T_2^{-1} in the ESR, NMR experiments. The actual values are consequences of a delicate balance between the self-energy and vertex corrections, which can modify the prefactors like $S(S+1)$ in Eq. (2)²³. Cancellation of that type are very well known in the scaling equation of the renormalized effective coupling, where the value of the spin S drops out²⁴. Considering the paramagnetic impurity electron-spin resonance that has been discussed earlier in detail²³ and it is found that in the T_2^{-1} relaxation rate the factor $(S+1)$ drops out. Thus the prefactor $S(S+1)$ in Eq. (2) may result in an essential overestimation for $S \geq 1$. A systematic study of that problem is not known in the present non-equilibrium situation²⁵. Therefore, the consequences of the present ambiguity is only demonstrated by introducing a multiplying factor λ of order of unity ($1/2 \leq \lambda \leq 2$) for the relaxation rate given by Eq. (2) and the role of λ will be discussed. It is reasonable to assume, that the factor λ imitating those cancellations is more important for larger spins $S > 1$.

In the following the logarithmic approach is applied for the non-equilibrium case, and the anomalous Korringa relaxation is additionally built in.

Considering the theoretical methods two ways can be followed: (i) The Keldysh Green function technique devoted to the non-equilibrium^{13,15,19} which may be combined with the non-crossing approximation²⁶. (ii) Direct calculation of the scattering rate by the time ordered perturbation theory starting with an arbitrary state and taking into account the actual distributions in the occupations of the intermediate and final states^{14,27}. Restricting to logarithmic accuracy the second method is very easy to apply, in other cases one should turn to the first one.

The paper is organized as follows. In Section II the transport phenomenon is imposed. In Section III the kernel in transport equation due to the magnetic impurity mediated electron-electron scattering is determined

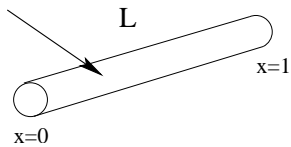


FIG. 1: The wire of length L . The arrow points to the position x of the attached tunnel junction which is measured in units of L .

using the leading logarithmic approximation. The electron distribution and exchange coupling renormalization is carried out in a self-consistent way. In Section IV the Korringa relaxation is taken into account in the kernel and in the smearing of the renormalized coupling, and then it is also determined in a self-consistent way with the other quantities. In Section V the results are analyzed from the point of view of the importance of the different ingredients of the theory. In the Conclusion the results obtained are summarized also from the point of view of Ref. 31, where the simplified method is applied for the case where the magnetic surface anisotropy¹⁸ is included.

II. NON-EQUILIBRIUM ELECTRON ENERGY DISTRIBUTION IN DIFFUSIVE WIRES

In the experiments the distribution of electron energies in a wire with large bias was measured at different position by attaching extra tunnel junction to the side of the wire (see Fig. 1). According to that we consider a wire with length L and the distribution function at position x in the wire in units of L for energy ε and at time t is denoted by $f(\varepsilon, x, t)$. The non-equilibrium distribution function in the diffusive limit is determined by the time dependent Boltzmann equation

$$\frac{\partial f(\varepsilon, x, t)}{\partial t} - \frac{1}{\tau_D} \frac{\partial^2 f(\varepsilon, x, t)}{\partial x^2} + I_{coll.}(\{f\}) = 0 \quad (3)$$

where $\tau_D = \frac{L^2}{D}$ is the diffusion time and D is the diffusion constant. In the followings the stationary solution is taken, thus the time dependence is dropped and f is assumed to be independent of the spin. The collision integral $I_{coll.}(\{f\})$ due to inelastic scatterings in Eq. (3) can be expressed by the scattering rate $W(\varepsilon, E)$ of electrons of energy ε with energy transfer E as

$$I_{coll.}(\{f\}) = \int dE \{ f(\varepsilon) [1 - f(\varepsilon - E)] W(\varepsilon, E) - [1 - f(\varepsilon)] f(\varepsilon - E) W(\varepsilon - E, -E) \}. \quad (4)$$

In absence of inelastic scattering processes $I_{coll.}(\{f\}) = 0$, thus the solution of Eq. (3) is a double-step distribution function²⁸

$$f^{(0)}(\varepsilon, x) = (1 - x)n_F(\varepsilon - \frac{eU}{2}) + xn_F(\varepsilon + \frac{eU}{2}) \quad (5)$$

where U is the voltage between the ends of the wire. The sharp steps are smeared due to the inelastic processes even at very low temperature. Taking into account inelastic scattering in W and starting with the solution Eq. (5), the Boltzmann equation can be solved self-consistently at least numerically.

In the numerical calculation searching for the stationary solution the Boltzmann equation is solved by iteration. In the iteration we start with the solution in absence of inelastic processes (Eq. (5)) and after at each step of the iteration the collision integral is calculated from the actual distribution function and scattering rate and then the new distribution function satisfying the boundary conditions is determined. The variables x and ε are discretized usually in 20-60 points. The number of the necessary iterations depends on the approximations used in the calculation of the collision integral, but usually the final solution is reached by 20-120 iteration.

For electron-electron interaction the scattering rate W can be expressed as

$$W(\varepsilon, E) = \int d\varepsilon' K(E, \varepsilon, \varepsilon') f(\varepsilon') [1 - f(\varepsilon' + E)] \quad (6)$$

where the kernel $K(E, \varepsilon, \varepsilon')$ is determined by the specific interaction and ε' is the energy after the collision.

The predicted dependence of the kernel K on E in case of the Coulomb electron-electron scattering¹⁰ is $\sim E^{-3/2}$ in $1D$ regime which explains perfectly some of the experiments⁸, but in other cases other relaxation mechanisms must exist. The Saclay group⁷ introduced phenomenologically an extra interaction between the electrons with $K \sim 1/E^2$ singularity. It is known since a long time²⁹ that the interaction mediated by magnetic impurities is singular in the energy transfer and recently Kaminski and Glazman¹¹ called the attention to similar $1/E^2$ singularity in the magnetic impurity mediated electron-electron interaction kernel in the leading order of perturbation in the Kondo coupling. At that time authors of Ref. [11,12,13,14,15,16] suggested that the energy exchange is mediated by Kondo impurities (magnetic and structural defects).

In the following we perform a systematic study of the Boltzmann equation (3) for electron-electron interaction mediated by Kondo impurities and the different approximations are built in step by step.

Assuming low concentration of the impurities we will use the single impurity Kondo model³⁰

$$H = \sum_{\mathbf{k}, \sigma} \varepsilon_{\mathbf{k}} a_{\mathbf{k}\sigma}^\dagger a_{\mathbf{k}\sigma} + J_0 \sum_{\substack{\mathbf{k}\mathbf{k}' \\ \sigma\sigma'}} \mathbf{S} a_{\mathbf{k}\sigma}^\dagger \boldsymbol{\sigma}_{\sigma\sigma'} a_{\mathbf{k}'\sigma'} \quad (7)$$

where $a_{\mathbf{k}\sigma}^\dagger$ creates a conduction electron with momentum \mathbf{k} , spin σ and energy $\varepsilon_{\mathbf{k}}$ measured from the Fermi level. The conduction electron band is taken with constant energy density ρ_0 for one spin direction, with a sharp and symmetric bandwidth cutoff D_0 , $\boldsymbol{\sigma}$ stands for the Pauli matrices, J_0 is the Kondo coupling, and \mathbf{S} is the spin operator of the impurity.

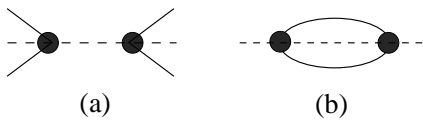


FIG. 2: The diagrams used for calculating (a) the kernel and (b) the Korringa lifetime of the impurity spin. The solid lines denote the conduction electrons, the dotted lines the impurity spin, and the blob is the Kondo coupling.

From perturbation theory in the coupling J_0 the first non-vanishing contribution to the kernel comes from the diagram in Fig. 2(a) as^{11,12}

$$K(E, \varepsilon, \varepsilon') = \frac{\pi}{2\hbar} \frac{c}{\rho_0} S(S+1) (2\rho_0 J_0)^4 \frac{1}{E^2} \quad (8)$$

where c is the concentration of the homogeneously distributed magnetic impurities in the wire. That kernel gives back the phenomenologically introduced energy dependence⁷, but its strength may be too small⁹ according to the small bare Kondo coupling J_0 .

III. LEADING LOGARITHMIC APPROXIMATION

To improve the calculation as the first step the renormalization of the coupling in the presence of the applied voltage is taken into account. The modified kernel reads

$$\begin{aligned} K(E, \varepsilon, \varepsilon') &= \frac{2\pi c}{\hbar} \rho_0^3 S(S+1) \times \\ &\times \left\{ \frac{2}{E^2} \left(S(S+1) [J(\varepsilon)J(\varepsilon'+E) - J(\varepsilon')J(\varepsilon-E)]^2 \right. \right. \\ &\quad \left. \left. + 2J(\varepsilon)J(\varepsilon')J(\varepsilon'+E)J(\varepsilon-E) \right) \right. \\ &\quad \left. - \frac{S(S+1)-1}{E(\varepsilon-\varepsilon'-E)} \left([J^2(\varepsilon) + J^2(\varepsilon')]J(\varepsilon'+E)J(\varepsilon-E) \right. \right. \\ &\quad \left. \left. - [J^2(\varepsilon-E) + J^2(\varepsilon'+E)]J(\varepsilon)J(\varepsilon') \right) \right\} \quad (9) \end{aligned}$$

where $J(\varepsilon)$ is the renormalized coupling and the approximations are made in spirit of logarithmic approximation discussed in detail in the Appendix. Considering only the most divergent terms proportional to $1/E^2$ in the limit $E \rightarrow 0$ and ignore the E -dependence in the arguments of J in Eq. (9) we get back the result of Eq. (14) of Ref.¹² thus the kernel is proportional to $J^2(\varepsilon)J^2(\varepsilon')/E^2$. The agreement with the result Eq. (10) of Ref. [11] is also only after taking the limit $E \rightarrow 0$ in J . In general, however, this factorization is not true, the kernel contains mixed terms as well.

In our non-equilibrium wire case the renormalized Kondo coupling depends also on the position x in the wire. In the leading logarithmic approximation carrying out similar resummation as in the equilibrium case, the

leading logarithmic scaling equation is

$$\frac{\partial J(\varepsilon, x)}{\partial(\ln \frac{D_0}{D})} = 2\rho_0 J^2(f(\varepsilon - D) - f(\varepsilon + D)) \quad (10)$$

where the original bandwidth cutoff D_0 is reduced to D . In Eq. (10) $|\varepsilon| \ll D$ is assumed, thus at the start the electron band can be taken always symmetric to ε , which assumption is not applicable in general. On the right hand side the actual distribution functions occur which must be determined in a self-consistent way. Assuming a single step like distribution that gives back the well known result²² and with a double step the ones in Ref. [14] and Ref. [16].

The renormalized Kondo coupling in the leading logarithmic approximation is the solution of Eq. (10):

$$J(\varepsilon, x) = \frac{J_0}{1 - 2\rho_0 J_0 \int_0^{D_0} \frac{dD'}{D'} (f(\varepsilon - D') - f(\varepsilon + D'))} \quad (11)$$

It is important to note that due to the finite voltage the width of the renormalized, resonant coupling $J(\varepsilon)$ is essentially reduced compared to the equilibrium values (see Fig.s 3 and 4), thus the logarithmic approach can be valid even well below the equilibrium Kondo temperature T_K for large bias U . Due to the finite voltage separate Kondo resonances are formed^{13,14,15,16} at the two Fermi energies corresponding to the two contacts thus $J(\varepsilon, x)$ has two peaks (see Fig.s 3 and 4). The validity of the logarithmic approach is restricted by the condition $\rho_0 J(\varepsilon, x) < 1$ nearby the two Fermi energies which was always checked in the calculation by plotting the actual Kondo coupling with respect to the energy.

In case of $eU > T_K$ the Kondo temperature is reduced and the singularity is smeared by the Korringa rate, thus the condition $\rho_0 J < 1$ is satisfied in most of the cases (see Fig.s 3 and 4).

In the numerical calculation $\rho_0 J(\varepsilon, x) > 1$ is replaced by $\rho_0 J(\varepsilon, x) = 1$ as $\rho_0 J(\varepsilon, x) > 1$ is always an artifact of the approximation.

IV. KORRINGA RELAXATION RATE

In the leading logarithmic order the self-energy corrections (wave function renormalization and Korringa lifetime²²) are neglected as they appear only in higher order. At a finite voltage U , however, that inverse lifetime proportional to U results in anomalous broadening which can be very essential. Therefore, the effect of U is taken into account in the spin spectral function $\rho_S(\varepsilon)$ by an energy independent Korringa lifetime τ_K as

$$\rho_S(\varepsilon) = \frac{1}{\pi} \frac{\frac{\hbar}{2\tau_K}}{\varepsilon^2 + \frac{\hbar^2}{4\tau_K^2}} \quad (12)$$

The energy dependence in τ_K leads to changes only in the tail of the spectral function which is independent of U for

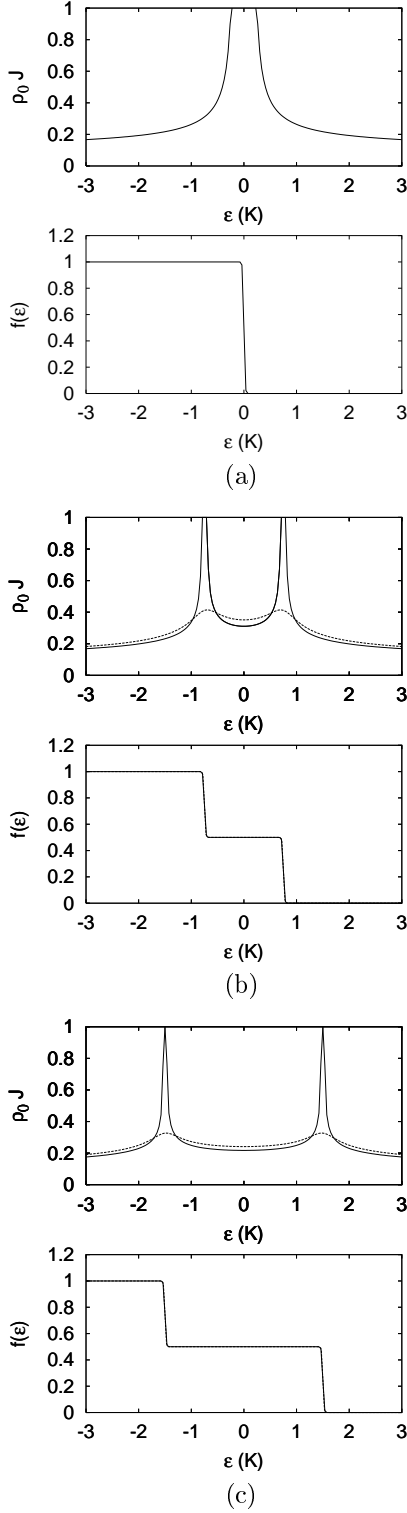


FIG. 3: The renormalized coupling (top) calculated from the sharp double-step distribution function (bottom) at $x = 0.5$; $T = 0.01$ K, $T_K = 0.15$ K ($\rho_0 J_0 = 0.039$, $D_0 = 5 \cdot 10^4$ K): (a) $U = 0$ mV, $\tau_K = \infty$ (b) $U = 0.15$ mV, solid line: $\tau_K = \infty$, dotted line: $\frac{\hbar}{2\tau_K} = 0.25$ K (c) $U = 0.3$ mV, solid line: $\tau_K = \infty$, dotted line: $\frac{\hbar}{2\tau_K} = 0.25$ K.

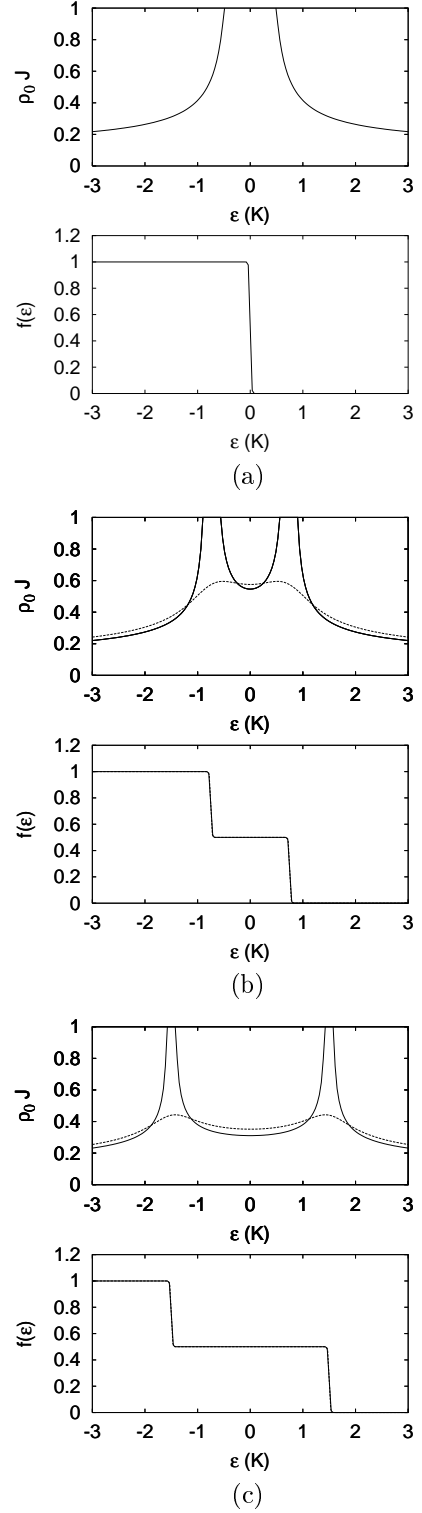


FIG. 4: The renormalized coupling (top) calculated from the sharp double-step distribution function (bottom) at $x = 0.5$; $T = 0.01$ K, $T_K = 0.3$ K ($\rho_0 J_0 = 0.042$, $D_0 = 5 \cdot 10^4$ K): (a) $U = 0$ mV, $\tau_K = \infty$ (b) $U = 0.15$ mV, solid line: $\tau_K = \infty$, dotted line: $\frac{\hbar}{2\tau_K} = 0.4$ K (c) $U = 0.3$ mV, solid line: $\tau_K = \infty$, dotted line: $\frac{\hbar}{2\tau_K} = 0.4$ K.

$|\omega| > eU$ and therefore it is neglected in the crude leading logarithmic approximation applied. The leading term of the Korringa relaxation rate is calculated according to the self-energy diagram in Fig. 2(b) as

$$\frac{1}{2\tau_K(x)} = \frac{2\pi}{\hbar} \rho_0^2 S(S+1) \int d\varepsilon J_K^2(\varepsilon, x) (1 - f(\varepsilon, x)) f(\varepsilon, x) \quad (13)$$

where in the self-consistent calculation the Korringa modified couplings J_K are used. In this way the effect of U and the position dependence are taken into account.

To include the effect of Korringa broadening the calculation of $K(E, \varepsilon, \varepsilon')$ given by Eq. (9) must be repeated using the spectral function Eq. (12) resulting in the following form of the kernel:

$$\begin{aligned} K(E, \varepsilon, \varepsilon', \tau_K) &= \frac{2\pi c}{\hbar} \rho_0^3 S(S+1) \times \\ &\times \left\{ \frac{2E^2}{(E^2 + \frac{\hbar^2}{4\tau_K^2})^2} \cdot \left(S(S+1) [J_K(\varepsilon)J_K(\varepsilon' + E) - J_K(\varepsilon')J_K(\varepsilon - E)]^2 \right. \right. \\ &\quad \left. \left. + 2J_K(\varepsilon)J_K(\varepsilon')J_K(\varepsilon' + E)J_K(\varepsilon - E) \right) \right. \\ &+ \frac{2\frac{\hbar^2}{4\tau_K^2}}{(E^2 + \frac{\hbar^2}{4\tau_K^2})^2} \cdot \\ &\quad \left. \left(S(S+1) [J_K(\varepsilon)J_K(\varepsilon' + E) + J_K(\varepsilon')J_K(\varepsilon - E)]^2 \right. \right. \\ &\quad \left. \left. - 2J_K(\varepsilon)J_K(\varepsilon')J_K(\varepsilon' + E)J_K(\varepsilon - E) \right) \right. \\ &+ \frac{(S(S+1) - 1)E(\varepsilon' - \varepsilon + E)}{(E^2 + \frac{\hbar^2}{4\tau_K^2})((\varepsilon' - \varepsilon + E)^2 + \frac{\hbar^2}{4\tau_K^2})} \cdot \\ &\quad \left([J_K^2(\varepsilon) + J_K^2(\varepsilon')]J_K(\varepsilon' + E)J_K(\varepsilon - E) \right. \\ &\quad \left. - [J_K^2(\varepsilon - E) + J_K^2(\varepsilon' + E)]J_K(\varepsilon)J_K(\varepsilon') \right) \\ &- \frac{(S(S+1) - 1)\frac{\hbar^2}{4\tau_K^2}}{(E^2 + \frac{\hbar^2}{4\tau_K^2})((\varepsilon' - \varepsilon + E)^2 + \frac{\hbar^2}{4\tau_K^2})} \cdot \\ &\quad \left([J_K^2(\varepsilon) + J_K^2(\varepsilon')]J_K(\varepsilon' + E)J_K(\varepsilon - E) \right. \\ &\quad \left. + [J_K^2(\varepsilon - E) + J_K^2(\varepsilon' + E)]J_K(\varepsilon)J_K(\varepsilon') \right) \left. \right\} \quad (14) \end{aligned}$$

where for the sake of simplicity we suppressed in the notation the spatial dependence of the kernel and the Kondo coupling. In Eq. (13) and (14) $J_K(\varepsilon)$ is the solution of the leading logarithmic scaling equation modified by the finite Korringa lifetime

$$\frac{\partial J_K(\varepsilon)}{\partial(\ln \frac{D_0}{D})} = 2\rho_0 J_K^2(\varepsilon) \int_{-\infty}^{\infty} d\varepsilon' \rho_S(\varepsilon - \varepsilon') (f(\varepsilon' - D) - f(\varepsilon' + D)). \quad (15)$$

The solution of Eq. (15) is the solution of the scaling equation Eq. (11) with infinite spin lifetime smeared by the spin spectral function as

$$J_K^{-1}(\varepsilon) = \int_{-\infty}^{\infty} d\varepsilon' \rho_s(\varepsilon - \varepsilon') J^{-1}(\varepsilon'). \quad (16)$$

Thus at each step of the iteration solving the Boltzmann equation the smeared, renormalized Kondo coupling $J_K(\varepsilon, x)$, the distribution function $f(\varepsilon, x)$, and the Korringa lifetime $\tau_K(x)$ were updated.

The spectral function given by Eq. (12) has further effects. In the most of the previous calculations the Korringa broadening is not taken into account (see e.g. Ref. [25]) in the initial and final states. It is easy to show that including those broadenings in the collision term can be taken into account as an additional broadening in the singular part of the kernel. As it has already been discussed in the Introduction the vertex corrections should reduce that broadening. Thus the broadening is intensified in that way, but after the reduction by the vertex corrections that cannot be very different from the overestimated one given by Eq. (13). At the end the amplitude of the relaxation rate is given by Eq. (13) and that modification is taken into account by a phenomenological factor λ ($1/2 \leq \lambda \leq 2$) and its influence on the results will be discussed later.

V. RESULTS AND DISCUSSION OF THE APPROXIMATIONS

In the numerical calculation at each step of the iteration the position dependent collision integral Eq. (4) is calculated in terms of the actual distribution function and the kernel defined in Eq. (6) in the following way: first the renormalized coupling J is calculated from the actual f smeared (Eq. (16)) or not (Eq. (11)) by the Korringa relaxation rate calculated from the preceding f and J . Then the new Korringa relaxation rate and after the kernel in terms of τ_K and J are calculated according to the Eqs (13) and (14). At the end of the given iteration step the new distribution function is determined from the old distribution function and the collision integral. The boundary conditions are satisfied at each step of the iteration by construction.

In the followings the results are presented and the importance of the different ingredients of the theory are analyzed.

A. Renormalized couplings

The renormalized couplings are calculated using Eq. (11) or (16) without and with the Korringa relaxation for different bias voltages. In Figs 3 and 4 the couplings calculated from the sharp double-step distribution function given by Eq. (5) are shown together with

the corresponding distribution functions. Without Korringa relaxation the resonances formed in the regions of the steps are very pronounced. Their widths can be interpreted as the renormalized Kondo temperature. For finite biases they are reduced due to the smaller steps with sizes x or $1 - x$ in the distribution function. The larger the bias the narrower the resonances are. At the overlap of the resonances the coupling can be essentially enhanced.

In Fig. 3(b) and (c) (Fig. 4(b) and (c)) just for demonstration a fixed value of the Korringa relaxation $\frac{\hbar}{2\tau_K} = 0.25\text{K}$ ($\frac{\hbar}{2\tau_K} = 0.4\text{K}$) is used. In reality the effect of the Korringa broadening is larger for larger bias as τ_K^{-1} is linear in U . As it can be seen in Figs 3(c) and 4(c) with $U = 0.3\text{mV}$ the peaks are almost completely smeared. In that case the coupling can be well approximated by a constant value $\rho_0\bar{J}$, but it is enhanced compared to the bare one, e.g. in Fig. 5(a) and (b) $\bar{J}/J_0 \sim 9$ and $\bar{J}/J_0 \sim 5.5$, respectively. In that case the Korringa broadening can be estimated according to Eq. (2). For $S = 1/2$, $x = 0.5$, $eU = 0.15\text{meV}$ and $\rho_0\bar{J} = 0.35$ ($eU = 0.3\text{meV}$ and $\rho_0\bar{J} = 0.23$) the relaxation rate is $\frac{\hbar}{2\tau_K} = 0.22\text{K}$ ($\frac{\hbar}{2\tau_K} = 0.19\text{K}$). For larger bias the dependence of the approximating constant coupling on the voltage is negligible (see Fig. 6). (That is the reason why the same values of $\frac{\hbar}{2\tau_K}$ were chosen in Fig. 5(a) and (b) for the different biases $eU = 0.15\text{meV}$ and $eU = 0.3\text{meV}$.) In this way the Korringa broadening can exceed the width of the resonance reduced by the bias and that can be so effective that the resonances disappear and the effect of the bias is only in the averaged coupling $\rho_0\bar{J}$. In this way the dependence of the final result on $\frac{\hbar}{2\tau_K}$ is very weak.

In Fig. 5 we show that the solution of the self-consistent calculation using the leading order renormalized coupling (solid line) can be well approximated by a constant coupling (dotted line). The parameters used in the calculation are $\tau_D = 1.8\text{ns}$, $c = 4\text{ppm}$, $\rho_0 = 0.21/(\text{site eV})$, $S = 1/2$, $T = 0.05\text{K}$, $T_K = 0.15\text{K}$.

Based on that observation, the approximation in which the self-consistent calculation is performed by using an appropriate constant value for the coupling is applied in Ref. [31] and Paper II where the surface magnetic anisotropy for the impurity spin is included.

It is important to note, however, that the approximating constant coupling depends on the voltage bias and on the bare coupling ($\sim T_K$). The former is illustrated in Fig. 6 for $T_K = 0.15\text{K}$.

The dependence of the distribution function on the impurity concentration is shown in Fig. 7 for (a) $U = 0.15\text{mV}$ and (b) $U = 0.3\text{mV}$ using the appropriate constant couplings obtained from Fig. 5. The concentration dependent correction is linear only for lower concentrations.

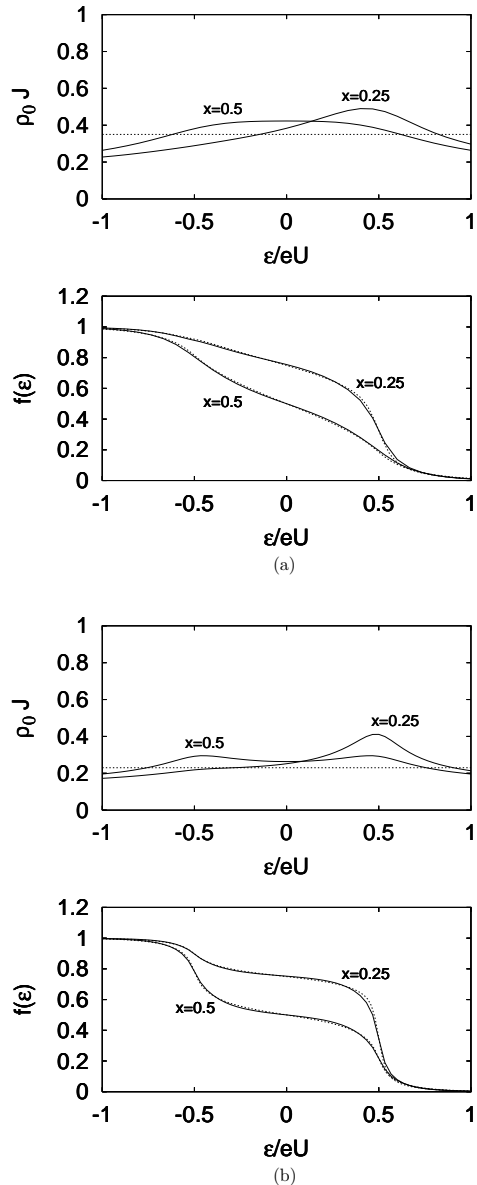


FIG. 5: The coupling constant (top) and the distribution function (bottom) obtained from the self-consistent calculation using the leading logarithmic renormalized coupling (solid line) and an appropriate constant coupling $\rho_0\bar{J}$ (dotted line). (a) $U = 0.15\text{mV}$, $\rho_0\bar{J} = 0.35$, (b) $U = 0.3\text{mV}$, $\rho_0\bar{J} = 0.23$. The other parameters are $\tau_D = 1.8\text{ns}$, $c = 4\text{ppm}$, $T_K = 0.15\text{K}$, $\rho_0 = 0.21/(\text{site eV})$, $S = 1/2$, $T = 0.05\text{K}$.

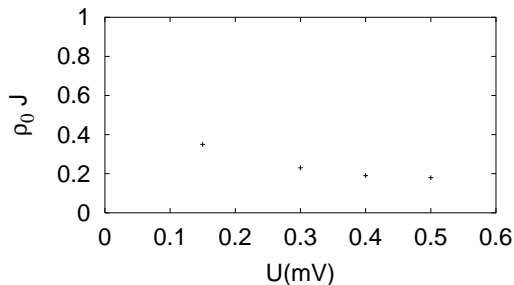


FIG. 6: The dependence of the averaged, approximating coupling $\rho_0\bar{J}$ on the voltage bias for $T_K = 0.15\text{K}$. The other parameters are $\tau_D = 1.8\text{ns}$, $c = 4\text{ppm}$, $\rho_0 = 0.21/(\text{site eV})$, $T = 0.05\text{K}$.

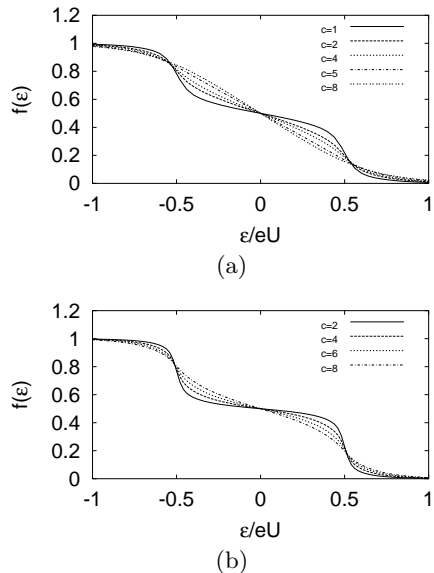


FIG. 7: The dependence of the distribution functions on the impurity concentration is illustrated using the appropriate constant couplings obtained (see Fig. 5). (a) $U = 0.15\text{mV}$, $\rho_0\bar{J} = 0.35$, (b) $U = 0.3\text{mV}$, $\rho_0\bar{J} = 0.23$. The other parameters are $\tau_D = 1.8\text{ns}$, $T_K = 0.15\text{K}$, $\rho_0 = 0.21/(\text{site eV})$, $T = 0.05\text{K}$.

B. Distribution function

The calculations are performed according to the iteration scheme described above. In case of $\tau_K = \infty$ the kernel given by Eq. (9) is singular in the energy transfer E as E^{-2} . There is, however, the cross term with the less singular denominator $E(\varepsilon - \varepsilon' - E)$. That term is less important because of the weaker singularity. Furthermore that drops out when the energy dependence of the couplings is neglected.

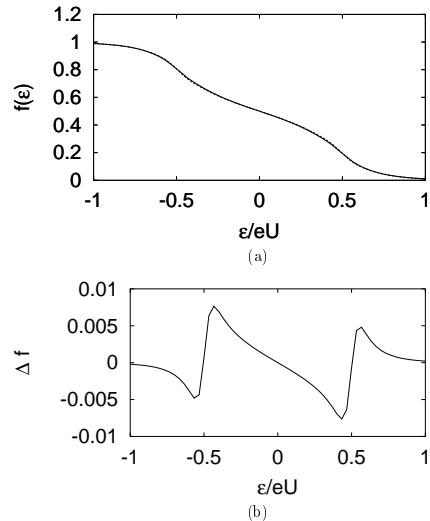


FIG. 8: Comparison of the solutions of the self-consistent calculation with and without the cross terms in the kernel Eq. (14). (a) the distribution functions with (solid line) and without the cross terms (dotted line) (b) the difference between the two solutions. $\tau_D = 1.8\text{ns}$, $c = 4\text{ppm}$, $\rho_0 = 0.21/(\text{site eV})$, $S = 1/2$, $x = 0.5$, $T = 0.05\text{K}$, $T_K = 0.3\text{K}$, $U = 0.3\text{mV}$.

In the presence of finite Korringa relaxation the situation is more complex (see the kernel given by Eq. (14)). The cross term does not disappear even for constant coupling, but it has limited importance as it is demonstrated by calculating the final distribution function without and with the cross term. In Fig. 8 the role of the cross terms in the kernel given by Eq. (14) is illustrated (a) where the solution of the self-consistent calculation is plotted with (solid line) and without the cross term (dotted line). The parameters used in the calculation are $\tau_D = 1.8\text{ns}$, $c = 4\text{ppm}$, $\rho_0 = 0.21/(\text{site eV})$, $S = 1/2$, $T = 0.05\text{K}$, $T_K = 0.3\text{K}$, $U = 0.3\text{mV}$, and $x = 0.5$. The difference is minor which can be seen from Fig. 8(b). Deviation occurs only in the vicinity of the steps. Thus in most of the cases neglecting of the cross terms is a good approximation.

C. The effect of the ambiguity in the strength of the Korringa relaxation

It has been pointed out earlier that the anomalously strong Korringa relaxation in the non-equilibrium case is not treated in a consequent way as the vertex corrections and the broadening of the initial and final states are not taken into account properly. In order to judge their importance a multiplicative factor λ is introduced as $\frac{\hbar}{2\tau_K} \rightarrow \lambda \frac{\hbar}{2\tau_K}$ (later the notation $\gamma = \lambda S(S+1)$ is used). Two sets of curves are calculated for biases 0.1mV

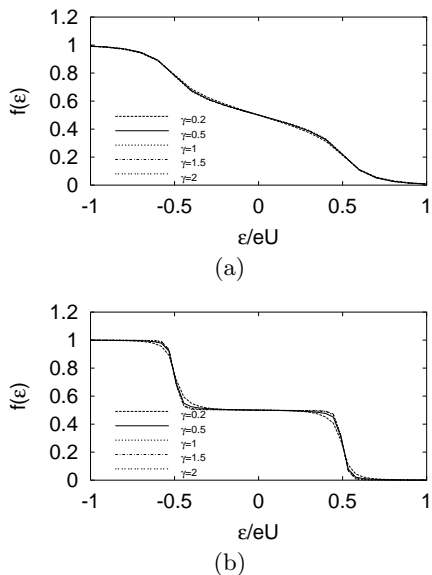


FIG. 9: The distribution functions are illustrated where the Korrington relaxation rates are modified by a multiplying factor; $\gamma = \lambda S(S + 1)$. (a) $U = 0.1\text{mV}$ (b) $U = 0.3\text{mV}$. The other parameters are $\tau_D = 2.8\text{ns}$, $c = 5\text{ppm}$, $\rho_0 = 0.21/(\text{site eV})$, $T_K = 0.3\text{K}$, $T = 0.05\text{K}$.

and 0.3mV (see Fig. 9). In both cases γ is changed in the wide interval $0.2 \leq \gamma \leq 2$. The differences are relatively very small as γ exceeds the value $\gamma \sim 0.4$. That is a consequence of the large smearing in the coupling and even more in the distribution function. Thus, the improper treatment of the vertex corrections is not expected to show up as drastic changes in the results.

D. Distribution function at points out of the middle

The calculation can be performed at any position in the wire and the results are demonstrated in Fig. 10. In these cases the reduction in the widths of the Kondo resonances are different at the two steps, namely at the smaller step it is more reduced. In the distribution function the height of the steps is asymmetric according to the actual value of x .

E. Scaling in terms of the applied voltage bias

Already in the early experiments⁷ the scaling with respect to the applied voltage has been observed, thus the distribution function at a given position x was described by a single variable function $f_x(\frac{\varepsilon}{eU})$. Since that time the validity of the scaling has played a central issue both in experimental⁹ and theoretical studies^{11,12,15}.

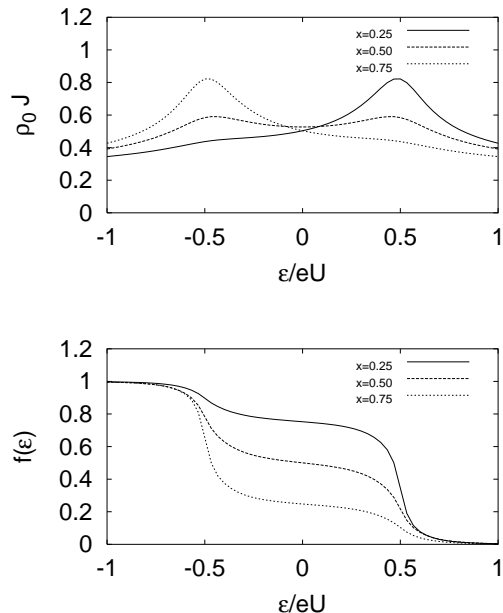


FIG. 10: The coupling constant (top) and the distribution function (bottom) obtained from the self-consistent calculation at different positions in the wire. The other parameters are $U = 0.3\text{mV}$, $\tau_D = 1.8\text{ns}$, $c = 4\text{ppm}$, $\rho_0 = 0.21/(\text{site eV})$, $T_K = 0.15\text{K}$, $T = 0.05\text{K}$.

In the present calculation the distribution function at position x is a function of the energy ε and voltage bias U and it is a functional of the self-consistently determined coupling $J(\varepsilon, eU; x)$, thus it can be written as $f_{\{J\}}(\varepsilon, eU; x)$. It has been demonstrated in Section V A that the coupling $J(\varepsilon, eU; x)$ is a slowly varying function of the energy for a fixed value eU in the relevant energy window with width eU , which is the dominant one concerning the non-equilibrium Boltzmann equation (3) case. Thus in case of slowly varying J shown in Figs 3, 4 and 5 the coupling $J(\varepsilon, x)$ can be approximated by an averaged one, $\bar{J}(eU)$ which is independent of x as it is also illustrated in Fig. 5. In that case the distribution function is simplified as $f_{\{J\}}(\varepsilon, eU; x) \Rightarrow f(\frac{\varepsilon}{eU}, \bar{J}(eU); x)$. Now, if J only slightly depends on the voltage bias U (see Fig. 6 for $T_K = 0.15\text{K}$) then the bias dependence can be dropped for a limited interval of eU and $\bar{J} = \text{const.}$ can be used. Then the distribution function is $f_{\{J\}}(\varepsilon, eU; x) \Rightarrow f(\frac{\varepsilon}{eU}, \bar{J}; x)$ which exhibits the scaling observed experimentally in several cases and illustrated in Fig. 11.

VI. CONCLUSION

In this paper the non-equilibrium transport is studied in the presence of magnetic impurities representing

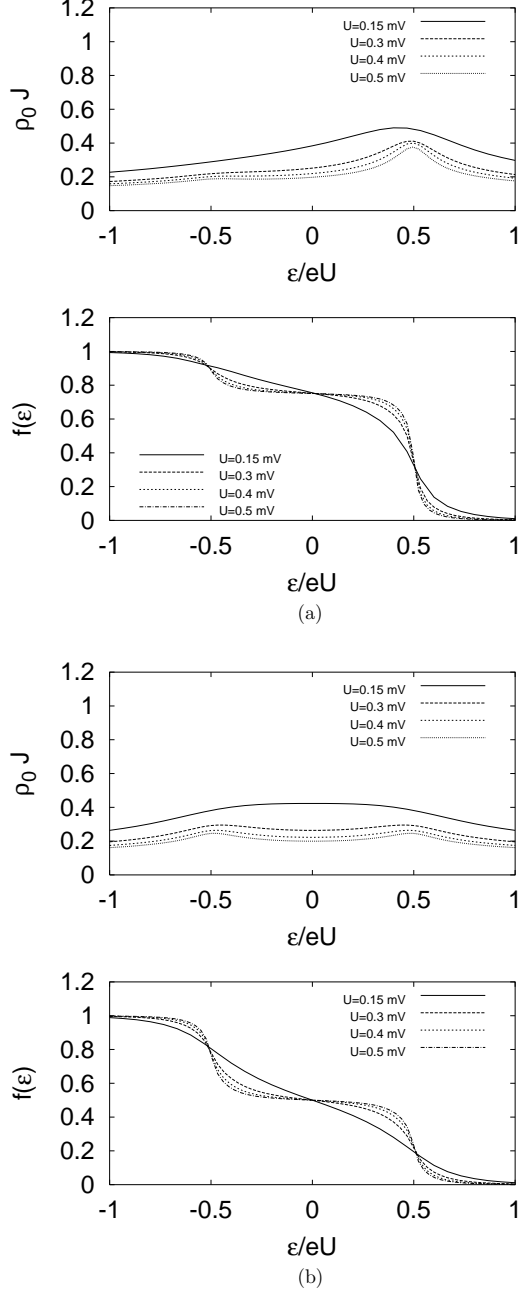


FIG. 11: The coupling constant (top) and the distribution function (bottom) obtained from the self-consistent calculation for different biases. (a) $x = 0.25$, (b) $x = 0.5$. The other parameters are $\tau_D = 1.8$ ns, $c = 4$ ppm, $T_K = 0.15$ K, $\rho_0 = 0.21/(\text{site eV})$, $T = 0.05$ K.

the 1-channel Kondo (1CK) problem. The results can be generalized to the 2CK problem which may be realized by dynamical structural defects³². In the logarithmic approximation scheme applied in the present paper there is no difference in the leading logarithmic order as the channel index silently follows the continuous electron line. The first differences occur in the next approxima-

tion as closed electron loops appear where summation is required with respect to the channel index, thus the Korrington relaxation and the vertex corrections are multiplied by the number of channels. As it has been discussed previously no drastic effects can be expected.

There is an other drawback of the application of the logarithmic approximation in the leading order as that overestimates the Kondo temperature by missing the prefactor $(2\rho_0 J)^{1/2}$. In general the contribution of the next to leading logarithmic approximation can be essential, but only nearby the Kondo temperature. The Korrington broadening reduces also that effect by reducing the averaged coupling $\rho_0 \bar{J}$. On the other hand if the Kondo temperature is comparable with the applied voltage, then the effective Kondo temperature is less reduced, thus the present method cannot be applied^{15,19}.

In the present scheme the kernel of the effective magnetic impurity induced electron-electron interaction is determined. That kernel is governed by the singularity E^{-2} in the energy transfer and the less singular cross term results only in minor changes. For determination of the distribution function a completely self-consistent calculation is carried out where in the framework of the ‘‘poor man’s’’ version of the renormalization group the couplings are modified by reducing the bandwidth which also modifies the Korrington rate and the electron distribution function.

For an arbitrary set of the parameters the distribution function can be determined using the method developed for the weak coupling limit, where T_K is small compared to the applied voltage. The relative importance of the different ingredients can be judged as the method is applied step by step. In the present formulation some details could be easier followed, than e.g. in the non-crossing approximation which is more powerful but many details are buried by the huge machinery.

Considering the comparison with the experiments an essential dilemma has been earlier realized. The required impurity concentration to fit the experiments in case of spin $S = 5/2$ magnetic impurities is in good accordance with values obtained by the other experiments determining the dephasing time. In contrary, the cases with presumable integer spins show drastic discrepancies. The dephasing requires sometimes less than one hundred of the impurity concentration and that was attributed to the surface anisotropy¹⁸ in Ref. 31.

The revised version of the form of the surface anisotropy¹⁸ makes the effect on the electron distribution much weaker, due to its smaller amplitude at larger distances measured from the surface. As in Ref. 31 it is shown that the surface anisotropy has weak effect on the shape of the distribution, thus the reduced number of impurities with large anisotropy very likely cannot change the distribution in an essential way.

Considering the dephasing rate, that effect may, however, be stronger, as the relevant energy range of the electrons is much smaller, as the applied voltage eU is replaced by the temperature ($eU > kT$). Thus, for more

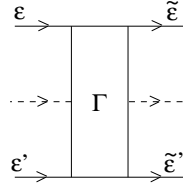


FIG. 12: The two electron and one pseudofermion scattering amplitude Γ . The solid and dotted lines represent the electrons and the pseudofermion, respectively. One of the electron lines connects continuously the upper corners in the amplitude Γ and the other the lower corners.

impurities, the anisotropy can dominate over the thermal energy, and the dephasing rate can be more reduced.

ACKNOWLEDGMENTS

We are grateful to N. O Birge, V. M. Fomin, H. Grabert, J. Kroha, H. Pothier, P. Wölfle, and G. Zaránd for useful discussions. This work was supported by Hungarian grants OTKA F043465, T046303, T048782, TS040878, T038162, grant No. RTN2-2001-00440, and MTA-NSF-OTKA Grant INT-0130446. One of us (A.Z.) thanks N. Andrei and P. Coleman for comments and the kind hospitality at Rutgers University.

APPENDIX

The derivation of the result Eq. (9) is outlined in the non-vanishing leading logarithmic order. The Abrikosov's pseudofermion technique³³ is applied where the b_α operators create spin states with index α and then $\mathbf{S} = \sum_{\alpha\beta} b_\alpha^\dagger \mathbf{S}_{\alpha\beta} b_\beta$. For simplicity the time ordered diagrams are used with real time. That technique can be applied starting with arbitrary states (e.g. non-equilibrium) and the transition amplitude between states $|i\rangle$ and $\langle f|$ is given as

$$\langle f|T|i\rangle_\omega = \sum_{n=1}^{\infty} \langle f|H_1 \left(\frac{1}{\omega + i\delta - H_0} H_1 \right)^n |i\rangle, \quad (\text{A.1})$$

where ω is the energy of the initial state.

The scattering rate can be calculated in two different ways: (i) The scattering amplitudes Γ are evaluated using Eq. (A.1) and then those are inserted in the golden rule. (ii) The imaginary part of the scattering amplitude is combined with the optical theorem (that method is used in Ref. 14).

In the first method the direction of the spin lines coincides with the time evolution as only one spin state can be present at a given time. In the second method the two electron scattering amplitude is determined like in the original work of Sólyom and Zawadowski²⁹ and the spin line is closed.

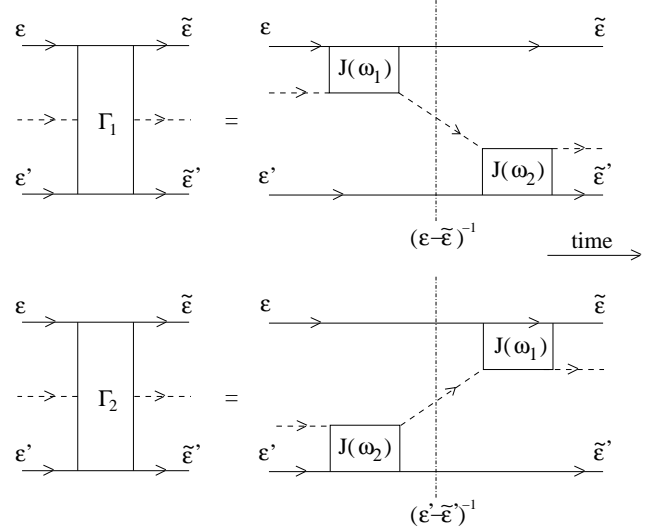


FIG. 13: The two basic diagrams providing singular terms in the energy transfer. The solid and dotted lines represent the electrons and the pseudofermion, respectively. The square box represents the logarithmic electron-pseudofermion vertex correction $J(\omega)$ and the dotted line the position of the energy denominator.

In the following the first method is used like in the papers by Kaminski and Glazman¹¹ and Göppert and Grabert¹². The two basic diagrams providing singular terms in the energy transfer $E = \varepsilon - \tilde{\varepsilon}$ can be seen in Fig. 13 where the logarithmic vertex corrections $J(\omega)$ with two electron and two pseudofermion legs are represented by square boxes. In these amplitudes the energy is conserved, thus $\varepsilon + \varepsilon' = \tilde{\varepsilon} + \tilde{\varepsilon}'$. The energy denominators indicated by dotted lines in Fig. 13 separate the two vertex corrections Γ_1 and Γ_2 and they are $\varepsilon - \tilde{\varepsilon} = E$ and $\varepsilon' - \tilde{\varepsilon}' = \tilde{\varepsilon} - \varepsilon = -E$ where in the latter the energy conservation is used. These are singular in the energy transfer E .

As in case of absence of magnetic field and surface anisotropy the spins do not carry energy and the incoming and outgoing electrons are on the energy shell, thus the energy variables of the vertices are $\omega_1 = \varepsilon$, $\omega_2 = \tilde{\varepsilon}' = \varepsilon + \varepsilon' - \tilde{\varepsilon} = \varepsilon' + E$ in Γ_1 and $\omega_2 = \varepsilon'$, $\omega_1 = \tilde{\varepsilon} = \varepsilon - E$ in Γ_2 . In terms of the energy dependent vertex $J(\omega)$ which is real in the logarithmic approximation the contributions are proportional to $J(\varepsilon)J(\varepsilon' + E)$ and $J(\varepsilon')J(\varepsilon - E)$, respectively.

Applying the golden rule the sum of the contributions of these two diagrams must be squared. In order to visualize the result of the detailed calculation we show the two forward scattering diagrams in Fig. 14 in the spirit of the optical theorem where the arrows indicate from where the imaginary parts are taken, thus the energy is conserved. Considering the second ‘‘crossing’’ diagram in the vertex on the right hand side the energy variables of the final states $\tilde{\varepsilon} \leftrightarrow \tilde{\varepsilon}'$ are interchanged in comparison to the first diagram (see Fig. 14). That results also in changing the

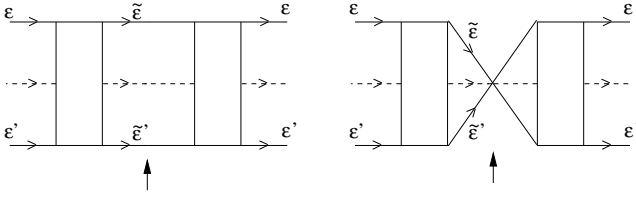


FIG. 14: The two forward scattering diagrams coming in the golden rule. The solid and dotted lines represent the electrons and the pseudofermion, respectively. The square boxes represents the appropriate vertexes (Γ_1 or Γ_2) and the arrows show from where the imaginary parts are taken.

energy denominators like $\varepsilon - \tilde{\varepsilon} = E \rightarrow \varepsilon - \tilde{\varepsilon}' = -\varepsilon' + \tilde{\varepsilon} = \varepsilon - \varepsilon' - E$ and $\varepsilon' - \tilde{\varepsilon}' = -E \rightarrow \varepsilon' - \tilde{\varepsilon} = -(\varepsilon - \varepsilon' - E)$

and also $\omega_2 = \varepsilon' + E \rightarrow \omega_2 = \tilde{\varepsilon} = \varepsilon - E$ in Γ_1 and $\omega_1 = \varepsilon - E \rightarrow \omega_1 = \varepsilon + \varepsilon' - \tilde{\varepsilon} = \varepsilon' + E$ in Γ_2 .

In the “non-crossing” term the energy denominators lead to a $1/E^2$ singularity. The vertex corrections corresponding to the terms proportional to Γ_1^2 , Γ_2^2 and $\Gamma_1\Gamma_2$ ($\Gamma_2\Gamma_1$) are $J(\varepsilon)^2J(\varepsilon' + E)^2$, $J(\varepsilon')^2J(\varepsilon - E)^2$ and $J(\varepsilon)J(\varepsilon' + E)J(\varepsilon')J(\varepsilon - E)$ occur in Eq. (9).

In the “crossing” contribution, however, the singularity has the form $(E(\varepsilon - \varepsilon' - E))^{-1}$. The corresponding vertex corrections are $J(\varepsilon)J(\varepsilon' + E)J(\varepsilon)J(\varepsilon - E)$, $J(\varepsilon)J(\varepsilon' + E)J(\varepsilon')J(\varepsilon' + E)$, $J(\varepsilon')J(\varepsilon - E)J(\varepsilon)J(\varepsilon - E)$, $J(\varepsilon')J(\varepsilon - E)J(\varepsilon')J(\varepsilon' + E)$ in the terms Γ_1^2 , $\Gamma_1\Gamma_2$, $\Gamma_2\Gamma_1$, and Γ_2^2 . The vertex corrections with these energy variables occur in Eq. (9), as well.

-
- ¹ P. Mohanty, E.M.Q. Jariwala, and R.A. Webb, Phys. Rev. Lett. **78**,3366 (1997); P. Mohanty and R.A. Webb, Phys. Rev. Lett. **84**, 4481 (2000).
- ² A.B. Gougam et al., J. Low Temp. Phys. **118**, 447 (2000); F. Pierre, Ann. Phys. (Paris) **26**, 4 (2001);
- ³ D. Natelson, R.L. Willett, K.W. West, and L.N. Pfeiffer, Phys. Rev. Lett. **86**, 1821 (2001).
- ⁴ F. Pierre et al. Phys. Rev. **B 68**, 085413 (2003); N.O. Birge and F. Pierre, in *Fundamental Problems of Mesoscopic Physics, Interaction and Decoherence* (Kluwer Academic, Dordrecht 2004), p. 3, cond-mat/0401182
- ⁵ F. Schopfer et al., Phys. Rev. Lett. **90**, 056801 (2003).
- ⁶ P. Mohanty, R.A. Webb, Phys. Rev. Lett. **91**, 066604 (2003).
- ⁷ H. Pothier et al. Phys. Rev. Lett. **79**, 3490 (1997); H. Pothier et al., Z. Phys. B: Cond. Mat. **104**, 178 (1997).
- ⁸ F. Pierre, H. Pothier, D. Esteve, and M.H. Devoret, J. Low Temp. Phys. **118**, 437 (2000).
- ⁹ F. Pierre et al., in *Kondo Effect and Dephasing in Low-Dimensional Metallic Systems* (Kluwer Academic, Dordrecht 2001), p. 119, cond-mat/0012038
- ¹⁰ B.L. Altshuler and A.G. Aronov, in *Electron-Electron Interactions in Disordered Systems*, Vol. 10 of Modern Problems in Condensed matter Sciences (North-Holland, New York, 1985), p. 1.
- ¹¹ A. Kaminski and L.I. Glazman, Phys. Rev. Lett. **86**, 2400 (2001).
- ¹² G. Göppert and H. Grabert, Phys. Rev. **B 64**, 033301 (2001).
- ¹³ J. Kroha, Adv. Solid State Phys. **40**, 267 (2000) and in *Kondo Effect and Dephasing in Low-Dimensional Metallic Systems* (Kluwer Academic, Dordrecht 2001), p. 133.
- ¹⁴ A. Zawadowski, in *Electronic correlations: From Meso- to Nano- Physics* (EDP Sciences, Paris, 2001), p. 301;
- ¹⁵ J. Kroha and A. Zawadowski, Phys. Rev. Lett. **88**, 176803 (2002).
- ¹⁶ G. Göppert et al., Phys. Rev. **B 66**, 195328 (2002); G. Göppert and H. Grabert, Phys. Rev. **B 68**, 193301 (2003).
- ¹⁷ A. Anthore et al., in *Electronic correlations: From Meso- to Nano- Physics* (EDP Sciences, Paris, 2001), p. 301; A. Anthore et al. Phys. Rev. Lett., **90**, 076806 (2003).
- ¹⁸ O. Újsághy, A. Zawadowski, and B.L. Gyorffy, Phys. Rev. Lett. **76**, 2378 (1996); O. Újsághy and A. Zawadowski, Phys. Rev. **B 57**, 11598 (1998); Recently L. Szunyogh pointed out an incorrect approximation of the integral in the final step, which is corrected and an oscillating behavior decaying by the third power of the distance of the impurity from the surface is found (O. Újsághy and A. Zawadowski, unpublished). That makes the role of the surface anisotropy much weaker, thus that might have only very weak effect on the electron distribution. Other source of the surface anisotropy has been recently suggested by B.L. Gyorffy, L. Szunyogh and G. Zaránd (unpublished), which has weaker decay rate, thus that may be more relevant.
- ¹⁹ E. Lebanon, and P. Coleman, cond-mat/0501001.
- ²⁰ A. Oguri, Phys. Rev. **B 64**, 153305 (2001), J. Phys. Soc. Jpn. **71**, 2969 (2002), **74**, 110 (2005); E. Lebanon, A. Schiller, Phys. Rev. **B 65**, 035308 (2001).
- ²¹ for quantum dot ($x = 1/2$) P. Coleman, C. Hooley, O. Parcellot, Phys. Rev. Lett. **86**, 4088 (2001).
- ²² J. Koringa, Physica (Amsterdam) **XVI**, 601 (1950).
- ²³ M.B. Walker, Phys. Rev. **176**, 432 (1968); Phys. Rev. **B 1**, 3690 (1970); see also W. Götze and P. Wölfle, J. Low Temp. Phys. **5**, 575 (1971).
- ²⁴ C. Fowler, A. Zawadowski, Solid State Commun. **9**, 471 (1971); A.A. Abrikosov, A. Migdal, J. Low Temp. Phys. **3**, 519 (1970).
- ²⁵ J. Paaske, A. Rosch, J. Kroha, and P. Wölfle, Phys. Rev. **B 70**, 155301 (2004); A. Rosch, J. Paaske, J. Kroha, and P. Wölfle, J. Phys. Soc. Jpn. **74**, 118 (2005).
- ²⁶ T. Fujii and K. Ueda, J. Phys. Soc. Jpn. **74**, 127 (2005).
- ²⁷ J. Paaske, A. Rosch, P. Wölfle, Phys. Rev. **B 69**, 155330 (2004); A. Rosch, J. Paaske, J. Kroha, and P. Wölfle, Phys. Rev. **B 90**, 076804 (2003).
- ²⁸ K.E. Nagaev, Phys. Lett. **A 169**, 103 (1992), Phys. Rev. **B 52**, 4740 (1995).
- ²⁹ J. Sólyom and A. Zawadowski, Phys. Letters **25A**, 91 (1967); Zeitschrift für Physik **226**, 116 (1969).
- ³⁰ J. Kondo, Prog. Theor. Phys. Osaka **32**, 37 (1964).
- ³¹ O. Újsághy, A. Jakovác, and A. Zawadowski, Phys. Rev. Lett. **93**, 256805 (2004).
- ³² see for recent references L. Borda, A. Zawadowski, and

G. Zaránd, Phys. Rev. **B 68**, 045114 (2003) and G. Zaránd,
cond-mat/0411348

³³ A.A. Abrikosov, Physics, **2**, 5 (1965).